Science Signaling
AAAS

www.sciencesignaling.org/cgi/content/full/5/227/ra41/DC1

Supplementary Materials for

Matrix Rigidity Controls Endothelial Differentiation and Morphogenesis of Cardiac Precursors

Kshitiz, Maimon E. Hubbi, Eun Hyun Ahn, John Downey, Junaid Afzal, Deok-Ho Kim, Sergio Rey, Connie Chang, Arnab Kundu, Gregg L. Semenza, Roselle M. Abraham, Andre Levchenko*

*To whom correspondence should be addressed. E-mail: alev@jhu.edu

Published 5 June 2012, *Sci. Signal.* **5**, ra41 (2012)
DOI: 10.1126/scisignal.2003002

This PDF file includes:

Other Supplementary Material for this manuscript includes the following:
(available at www.sciencesignaling.org/cgi/content/full/5/227/ra41/DC1)

Movies S1 to S4 (.mp4 format). Dynamics of cell network formation from CDC spheroid aggregates.

Text S1.

ODE based mathematical model

We developed a mathematical model to simulate MRS induced changes in CDC fate. 4 distinct cell subpopulations within CDC population were considered: putative stem cells (ckit+/CD31-) denoted by N^{+-}, endothelial progenitor cells (ckit+/CD31+) denoted by N^{++}, differentiated endothelial cells (ckit-/CD31+) denoted by N^{-+}, and the remaining cells (ckit-/CD31-) denoted by N^{--}. We assumed that ckit+/CD31- cells can differentiate into ckit+/CD31+ cells, that can differentiate into ckit-/CD31+ cells, and that no other endothelial differentiation path exists. We also assumed that any apoptosis of ckit+/CD31-, and ckit+/CD31+ cells would be negligible as compared to the proliferation, or could be incorporated within their respective self renewal rates. The kinetic equations are:

$$\frac{d\ (N^{+-})}{dt} = \mathrm{k}_{+-}^{prolif} \times N^{+-} - k_{+-}^{diff} \times N^{+-}$$

$$\frac{d\ (N^{++})}{dt} = \mathrm{k}_{++}^{prolif} \times N^{++} + k_{+-}^{diff} \times N^{+-} - k_{++}^{diff} \times N^{++}$$

$$\frac{d\ (N^{-+})}{dt} = \mathrm{k}_{++}^{diff} \times N^{++} - k_{-+}^{apop} \times N^{-+}$$

$$\frac{N^{+-} + N^{++} + N^{-+} + N^{++}}{\sum_i N^i} = 1$$

The normalization of cell numbers in each subpopulation to add up to 1 (the last equation above) was performed in part to facilitate comparison to flow cytometry data.

For simulations, initial values for the distribution of cell subpopulations, N^i were kept consistent with the flow cytometry experimental data displayed in Fig. 2Q of the main text (k1$= 0.8\,day^{-1}$, k2$= 0.03\,day^{-1}$, k3$= 0.4\,day^{-1}$, k4$= 0.1\ day^{-1}$).

$$\frac{N^{+-}}{\sum_i N^i} = 0.08,\ \frac{N^{++}}{\sum_i N^i} = 0.00,\ \frac{N^{-+}}{\sum_i N^i} = 0.00,\ \frac{N^{--}}{\sum_i N^i} = 0.92\ .$$

Kinetic parameters were determined by selecting the best parameters that fit the experimental data in Fig. 2Q, unless indicated otherwise.

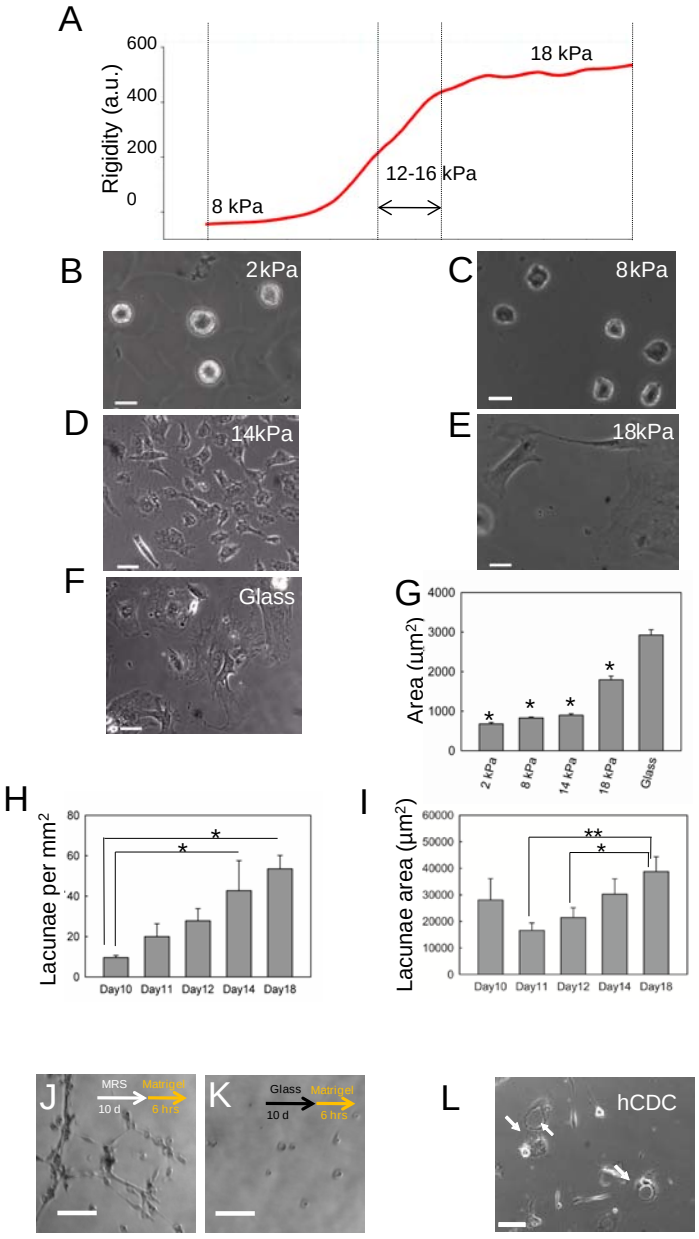

Figure S1. Substratum rigidity influences single-cell shape and multicell organization of CDCs. (A) Visualization of the rigidity profile of polyacrylamide (PAAM) gel in Fig. 1B, with higher rigidity values coinciding with higher fluorescence intensities for Alexa Fluor 594 hydrazide. (B-G) CDCs assume different morphologies on spatially homogeneous, fibronectin-coated polyacrylamide substrata of different rigidity values: 2 kPa (B), 8 kPa (C), 14 kPa (D), 18 kPa (E), and glass (F). Scale bar = 50 µm. (G) Single cell area of CDCs cultured on substrata of different rigidities after 3 days of culture. n = 3 samples, containing > 100 cells each. (H) Change in density of lacunae in the cellular networks over time. (I) Change in the percentage of the cultured area on MRS covered by lacunae formed by CDCs. (J-K) Lacunae formation by CDCs

cultured on glass (J) or MRS (K) for 10 days and transferred to Matrigel for 6 hours. Scale bar = 50 μm. (L) CDCs derived from human endomyocardial biopsy generate self-contained single cell loops similar to those formed by endothelial cells after 3 days of culture (see arrow). Scale bar = 100 μm. In all panels, *, $P < 0.05$; ***, $P < 0.001$ determined by Tukey's HSD test. For G, H, I, one-way ANOVA produced $P < 0.05$. Error bars represent standard error of mean (s.e.m).

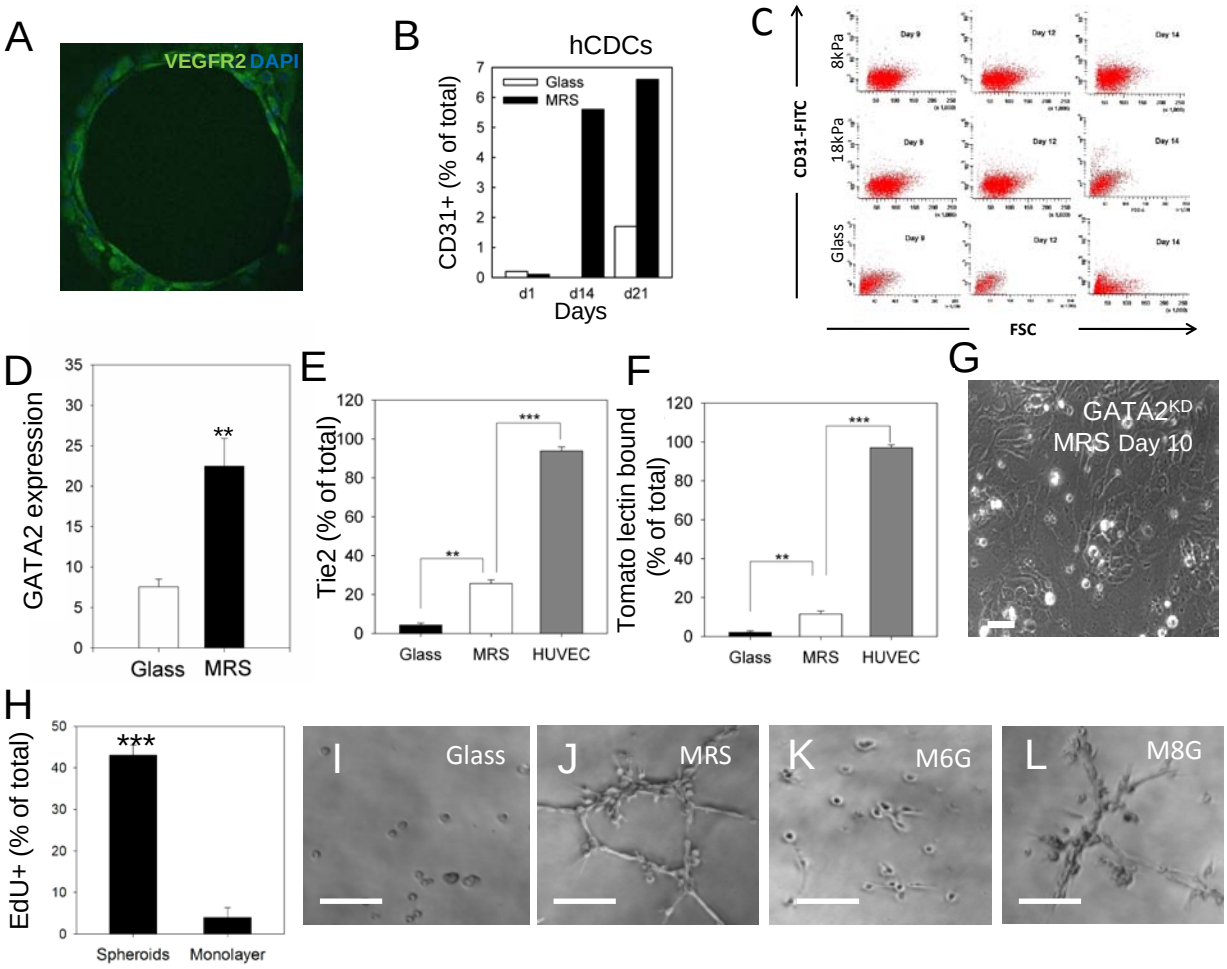

Figure S2. MRS promotes CDC proliferation and endothelial differentiation. (A) Confocal image of cells lining lacunae formed after 12 days of culture on MRS, showing the abundance of VEGFR2 (green). The nuclear stain DAPI is shown in blue. Scale bar = 50 μm. (B) Flow cytometry analysis of the percentage of $CD31^+$ subpopulation in human CDCs cultured on glass and MRS. (C) Flow-cytometric analysis of $CD31^+$ CDCs cultured for 9, 12, and 14 days on PAAM substrata of different rigidities (8 kPa, 18 kPa, or glass). (D) Quantitative comparison of GATA2 abundance (normalized to GAPDH abundance) in CDCs cultured on glass or MRS for 7 days. n = 3 experiments. (E-F) Culturing CDCs on MRS enhances the emergence of a subpopulation with endothelial-specific markers. Flow cytometry analysis of Tie2 abundance in cells cultured on glass or MRS for 14 days (E). Flow cytometry analysis of bound tomato lectin in CDCs cultured on glass or MRS for 14 days (F). HUVEC control shown in red. n = 3 cultures.

(G) Phase-contrast image of GATA2-shRNA transduced cells cultured for 10 days on MRS exhibiting monolayer morphology with no lacuna or cell network formation (n > 10). (H) Quantification of percentage of EdU^+ cells in monolayer or in spheroids formed after 7 days of culture on MRS (see Fig. 3A). n = 3 samples. (I-L) A persistent rigidity cue is required by CDCs to maintain potential for morphogenesis in Matrigel (n = 3 cultures). Phase-contrast images of CDCs seeded in Matrigel for 6 hours after culture on glass for 10 days (I), on MRS for 10 days (J), on MRS for 6 days followed by on glass for 4 days (M6G) (K), on MRS for 8 days followed by on glass for 2 days (M8G) (L). Scale bar, 100 μm for I-L. In all panels, **, $P< 0.01$; ***, $P<0.001$. P values calculated with Student-t-tests. Error bars represent standard error of mean (s.e.m).

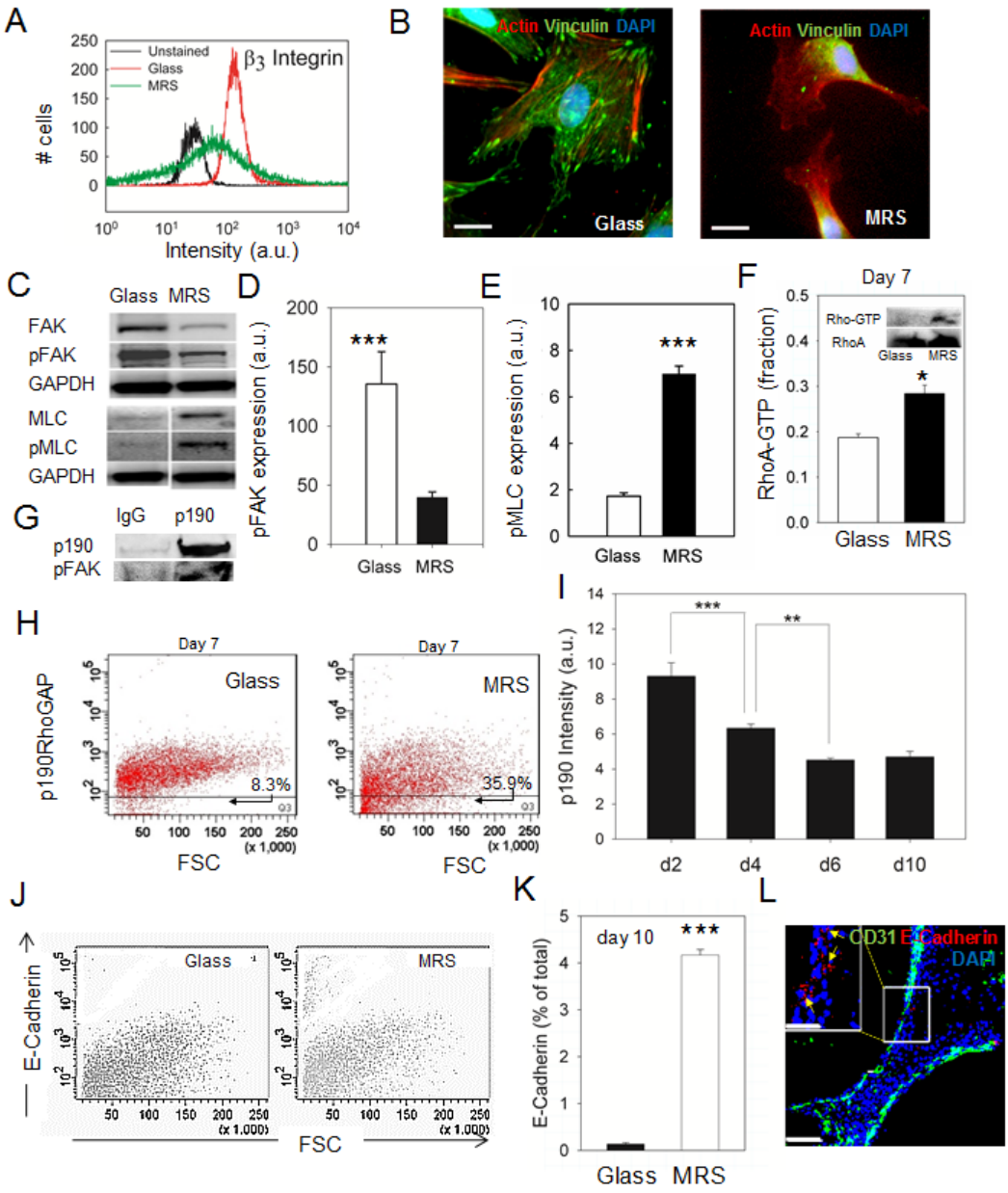

Figure S3. MRS influences cell-substratum and cell-cell interaction dynamics in CDC cultures. (A) Flow cytometry analysis of β_3 integrin in cells cultured for 3 days on glass (red), and MRS (green). Unstained sample is shown in black. (B) Staining for actin (red), and vinculin (green) reveals actin stress fibers and vinculin band formation in CDCs cultured on glass for 3 days (left), and the presence of a cortical actin cytoskeleton and lower abundance of vinculin in CDCs cultured on MRS for 3 days (right). Nuclei are stained with DAPI. Scale bar = 25 µm. (C-E) Immunoblotting analysis of focal adhesion kinase (FAK), phosphorylated FAK (pFAK), myosin light chain (MLC), and phosphorylated MLC (pMLC) in cells cultured for 7 days on glass (left lanes) or MRS (right lanes). GAPDH was the loading control (bottom) (C). Immunoblotting was run on non-contiguous lanes. Quantitative comparison of pFAK (D) and pMLC (E) abundance (normalized to GAPDH abundance). n = 3 experiments. (F) Immunoblot analysis of the ratio of RhoA-GTP and total RhoA abundances (immunoprecipitation bands

shown in inset). (G) Coimmunoprecipitation analysis reveals that pFAK interacts with p190RhoGAP (n = 3 samples). (H) Flow cytometry analysis of p190RhoGAP abundance in CDCs cultured for 10 days on glass and MRS. (I) Time course quantification of p190RhoGAP abundance in cells cultured on MRS (see Fig. 4F). n = 3 experiments. (J-K) The effect of culture on MRS on E-cadherin localization. Distribution of E-cadherin^{+} cells in cells cultured for 10 days on glass and MRS (J). Analysis of the percentage of E-cadherin^{+} cells (K). (L) Confocal image of CDCs cultured for 12 days on MRS revealing the presence of E-cadherin (red) in puncta (see arrows in the inset), with CD31 (green) and nuclei (DAPI) are also visualized. Scale bar = 50 μm and 100 μm for the inset. In all panels, *, $P < 0.05$; **, $P< 0.01$; ***, $P<0.001$. P-values were calculated by using Student-t-tests. Error bars represent standard error of mean (s.e.m)).

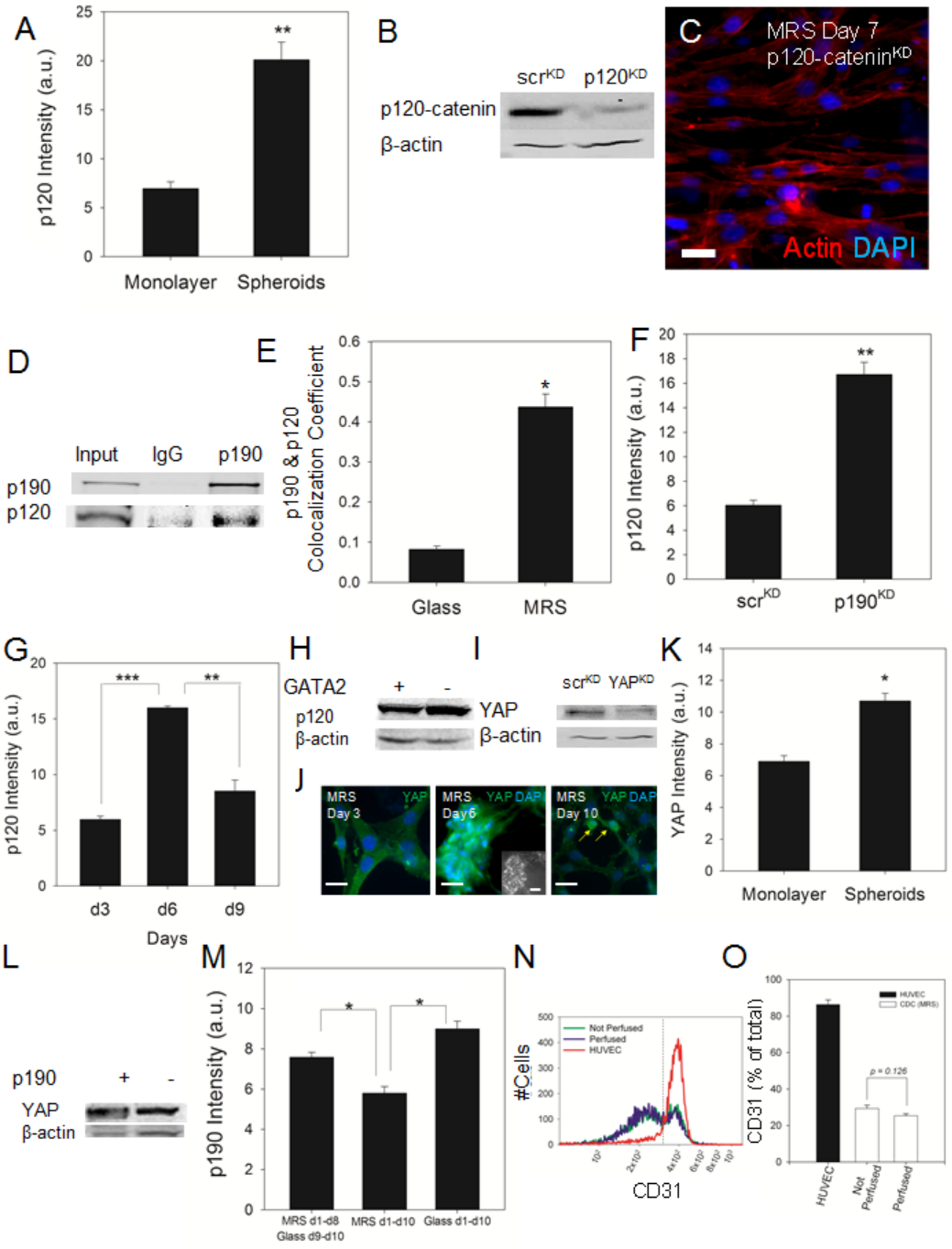

Figure S4. p190RhoGAP mediates cell-cell interaction in aggregate formation by regulating p120-catenin and YAP abundance and localization. (A) Quantification of immunoblotting analysis of p120-catenin in monolayer or in spheroids formed by cells cultured on MRS for 7 days (see Fig. 5A). n = 3experiments. (B) Immunoblot analysis of p120-catenin in CDCs lentivirally transduced with scrambled shRNA (scr^{KD}) or shRNA targeting p120-catenin ($p120^{KD}$) (top). β-actin was the loading control (bottom). n = 4 samples. (C) 2-photon microscopy of $p120^{KD}$ cells cultured on MRS for 6 days reveals lack of spheroid formation and

polarized morphology and actin cytoskeleton (red). n = 3 cultures. Scale bar = 100 μm. (D) Coimmunoprecipitation of p190RhoGAP with p120-catenin (right lane). Pull down with IgG was the control (center lane). (E) Quantification of colocalization of p190RhoGAP and p120-catenin in CDCs cultured on glass or MRS for 7 days (see Fig. 5B). n = 3 experiments. (F) Quantification of immunoblotting analysis of p120-catenin abundance in scr^{KD} control and $p190^{KD}$ cells (see Fig. 5C). n = 3 cultures. (G) Quantification of immunoblotting analysis of p120-catenin abundance in cells cultured on MRS for 3, 6, and 9 days (see Fig. 5D). n = 3 cultures. (H) Analysis of p120-catenin abundance in cells lentivirally transduced with scrambled (+) or GATA2 shRNA (-). β-actin was the loading control (bottom). (I) Immunoblot analysis of YAP in cells lentivirally transduced with scrambled (scr^{KD}) or YAP (YAP^{KD}) shRNA. β-actin was the loading control (bottom). (J) Immunostaining of YAP (green) in CDCs cultured on MRS over the course of 10 days reveals low nuclear localization of YAP by day 3, an increase to predominantly nuclear localization in spheroids by day 6 (also see 2-photon image in Fig. 5I-J), and reduced nuclear localization by day 10. The nuclear stain DAPI is blue. Scale bar = 20 μm. (K) Quantification of immunoblot analysis of YAP abundance in monolayers or spheroids formed after 7 days of culture of CDCs on MRS (see Fig. 5H). n = 3 cultures. (L) Immunoblot analysis show 27.3% increase in YAP abundance (n = 3 cultures, $p < 0.05$) in cells lentivirally transduced with scrambled (+) or p190RhoGAP shRNA (-).β-actin was the loading control (bottom). (M) Quantification of immunoblot analysis of p190RhoGAP abundance in CDCs cultured on MRS for 8 days followed by a 2 day culture on glass, or cells cultured on MRS and glass for 10 days (see Fig. 5L). n = 3 experiments. Significance determined by one-way ANOVA ($p < 0.05$). P values shown as determined by Tukey's HSD test. (N-O) Flow cytometry analysis of CD31 abundance in cells cultured on MRS for 14 days with a medium change every 3 days (Not perfused, green) or every 8 hours (perfused, blue). HUVEC control shown in red (N); Quantification of percentage of $CD31^{+}$ cells in Fig. S4N (O). In all panels, (*, $P < 0.05$; **, $P< 0.01$; ***, $P< 0.001$. P values calculated with Student-t-tests, unless otherwise mentioned. Error bars represent standard error of mean (s.e.m).

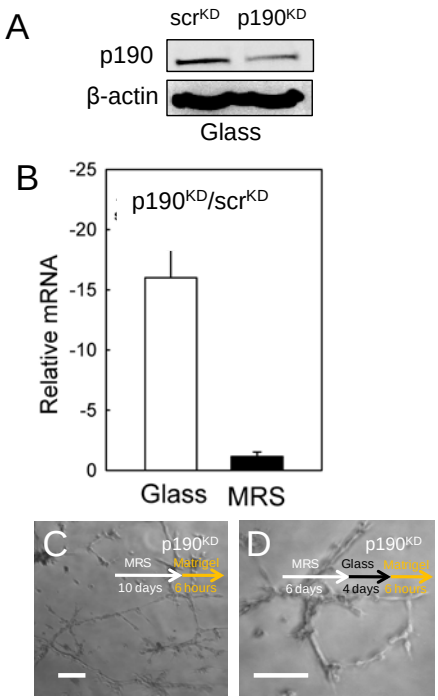

Figure S5. Characterization of p190RhoGAP-shRNA transduction. (A) Immunoblot analysis of p190RhoGAP in cells lentivirally transduced with scrambled and p190RhoGAP shRNA, measured 4 days after transduction. Lower panel shows β-actin abundance. (B) RT-PCR analysis of relative *p190RhoGAP* expression in $p190^{KD}$ CDCs compared to scr^{KD} CDCs cultured on glass (left bar), and in $p190^{KD}$ cells compared to scr^{KD} cells cultured on MRS (right bar). n=3 cultures. (C-D) p190RhoGAP silencing enables morphogenesis into lacunae networks even without a persistent extracellular rigidity cue (see Fig. S2, K-N). Phase-contrast images of $p190^{KD}$ CDCs seeded in Matrigel for 6 hours after 10 days of culture on MRS (C) or 6 days of culture on MRS followed by 4 days on glass (D). n = 3sets of CDCs for (C) and (D). Scale bar = 100 μm.

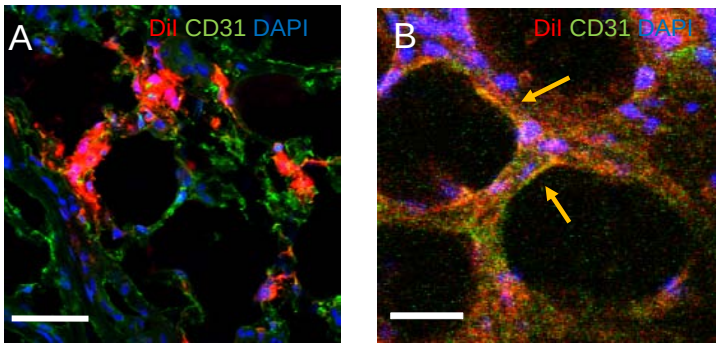

Figure S6. CDCs integrate in blood vessels in rat hearts. (A) Cardiosphere-derived cells (CDCs) labeled with DiI (red) integrate into blood vessels and are positive for CD31 (13% of sections analyzed, n = 24) in the host myocardium of a rat heart within 5 weeks of injection. (B) $p190^{KD}$ CDCs labeled with DiI (red) integrate in host myocardium of a rat heart after 5 weeks of injection (60% of sections analyzed, n = 6). DAPI is a nuclear stain. Scale bar = 50 μm.

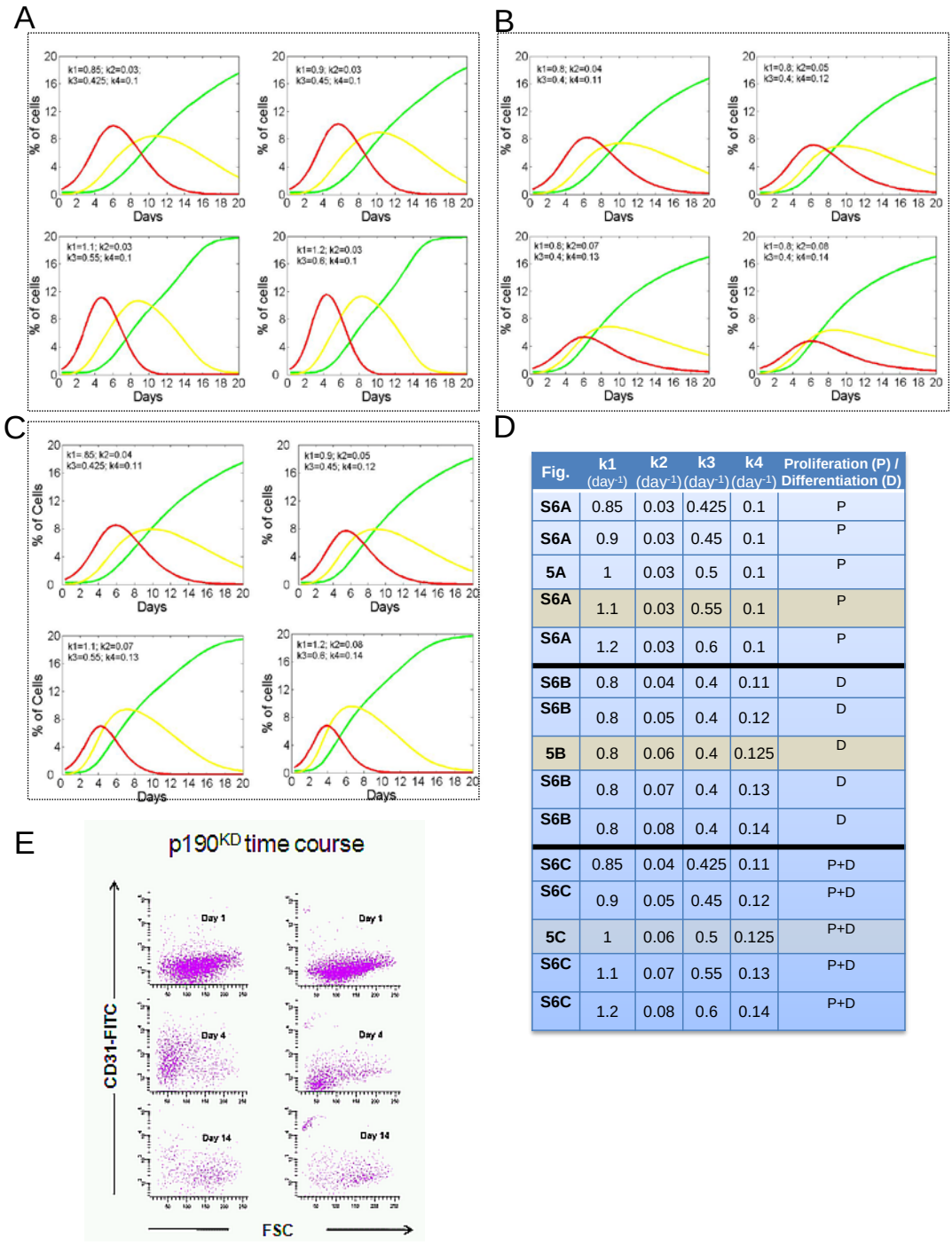

Fig.	k1 (day^{-1})	k2 (day^{-1})	k3 (day^{-1})	k4 (day^{-1})	Proliferation (P) / Differentiation (D)
S6A	0.85	0.03	0.425	0.1	P
S6A	0.9	0.03	0.45	0.1	P
5A	1	0.03	0.5	0.1	P
S6A	1.1	0.03	0.55	0.1	P
S6A	1.2	0.03	0.6	0.1	P
S6B	0.8	0.04	0.4	0.11	D
S6B	0.8	0.05	0.4	0.12	D
5B	0.8	0.06	0.4	0.125	D
S6B	0.8	0.07	0.4	0.13	D
S6B	0.8	0.08	0.4	0.14	D
S6C	0.85	0.04	0.425	0.11	P+D
S6C	0.9	0.05	0.45	0.12	P+D
5C	1	0.06	0.5	0.125	P+D
S6C	1.1	0.07	0.55	0.13	P+D
S6C	1.2	0.08	0.6	0.14	P+D

Figure S7. Model simulation of cell proliferation and differentiation. (A) Model simulation for different rates of proliferation for c-kit$^+$ and c-kit$^+$/CD31$^+$ cells (see Fig. 7A). (B) Model simulation for different rates of differentiation for c-kit$^+$/CD31$^-$, c-kit$^+$/CD31$^+$, and c-kit$^-$/CD31$^+$ subpopulations (see Fig. 7B). (C) Model simulation for CDC proliferation and differentiation showing the temporal distribution of c-kit$^+$/CD31$^-$, c-kit$^+$/CD31$^+$, and c-kit$^-$/CD31$^+$ subpopulations with different rates of both proliferation and differentiation for c-kit$^+$ and c-kit$^+$/CD31$^+$ cells (see Fig. 7C). (D) Parameters indicated refer to the model described in text S1.

(E) Flow cytometry analysis of c-kit and CD31 abundance in p190KD CDCs cultured on MRS over 14 days (cf. Fig. 7D).

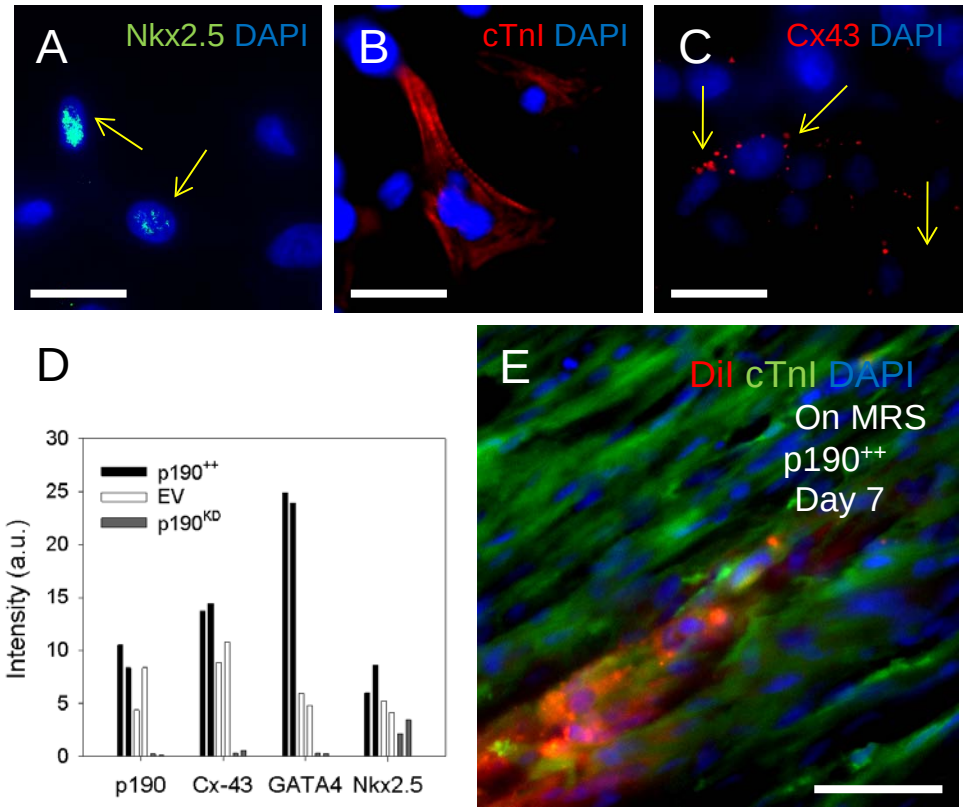

Figure S8. Increase in p190RhoGAP abundance promotes myocardial differentiation of CDCs. (A-C) Immunostaining of $p190^{++}$ CDCs cultured on glass for 7 days for Nkx2.5 (A), cardiac troponin I (cTnI) (B), and connexin-43 (C). The nuclear stain DAPI is shown in blue. Scale bar = 20 μm. (D) Immunoblot analysis of p190RhoGAP, connexin-43 (Cx-43), GATA4, and Nkx2.5 abundance in cells lentivirally transduced with empty sv40 vector (EV), p190RhoGAP overexpression vector ($p190^{++}$), and shRNA against p190RhoGAP (p190KD). Intensities were normalized to β-actin intensities. n = 2 samples (shown as separate bars). (E) Confocal image showing DiI (red) labeled $p190^{++}$ CDCs cultured on glass for 7 days and injected in rat heart. n = 3 slides. These CDCs are positive for cTnI (green) and integrate in host myocardium 7 days after injection. The nuclear stain DAPI is shown in blue. N = 3 slides from 1 animal. Scale bar = 50 μm.

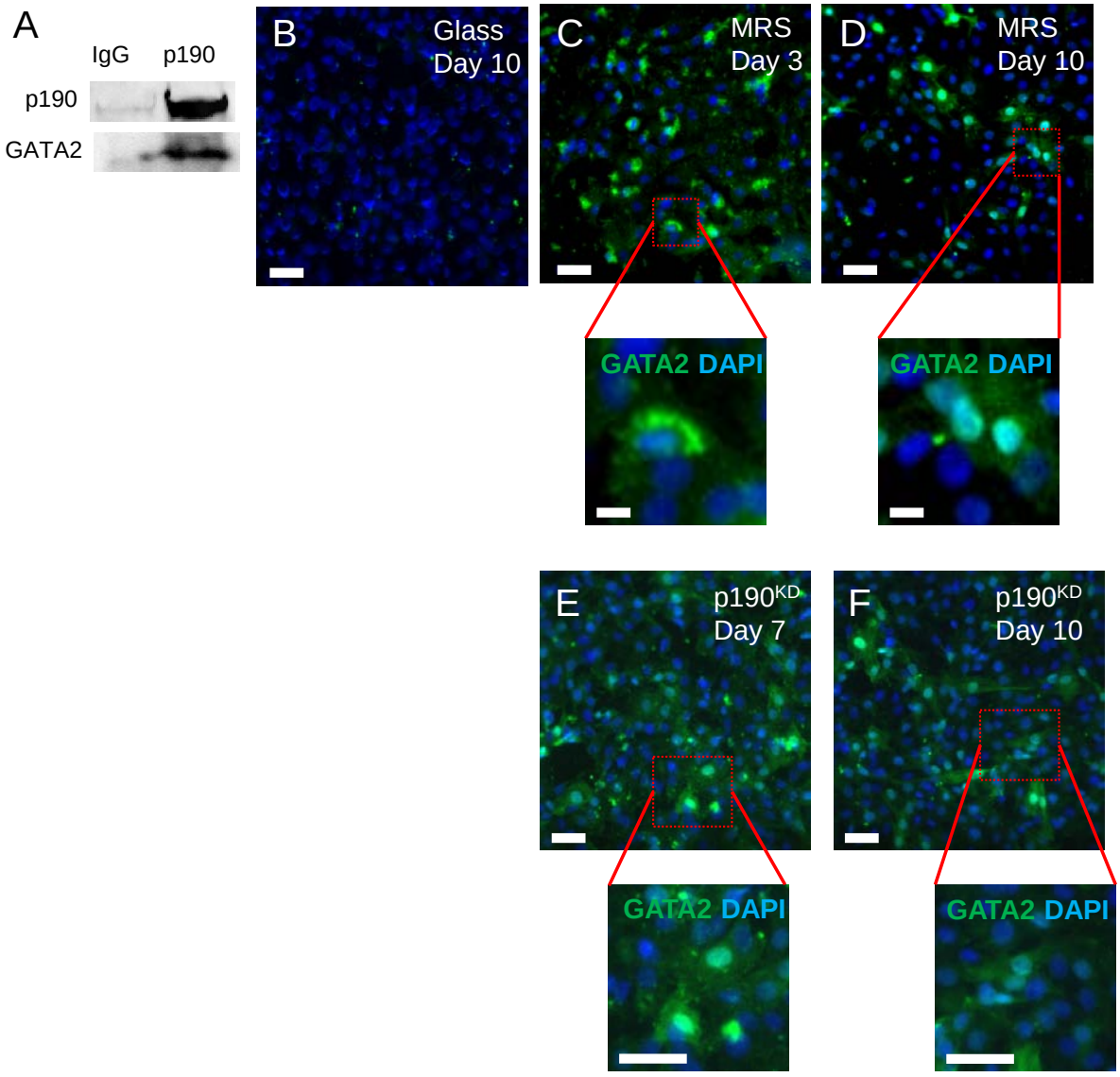

Figure S9. p190RhoGAP sequesters GATA2 in the cytosol. (A) Co-immunoprecipitation analysis of p190RhoGAP and GATA2. IgG control is shown in the left lane. n=2 experiments. (B-D) GATA2 localization in cells cultured on MRS (see also Fig. 9, A to E). Immunofluorescence images of CDCs cultured on glass for 10 days and stained for GATA2 (green) and Hoechst (blue) show peri-nuclear localization of GATA2 in CDCs after 10 days of culture on glass (B) and on MRS for 3 days (see magnification) (C), and nuclear localization (see magnification) in CDCs cultured on MRS for 10 days (D). Scale bar = 20 µm. n = 136 cells per condition. (E-F) Immunofluorescence images of $p190^{KD}$ CDCs cultured on MRS and stained for GATA2 (green), and Hoechst (blue) show both nuclear and peri-nuclear localization for GATA2

after 3 days (E), and mostly nuclear localization after 10 days of culture (F). n = 242 cells per condition. Scale bar = 20 μm.

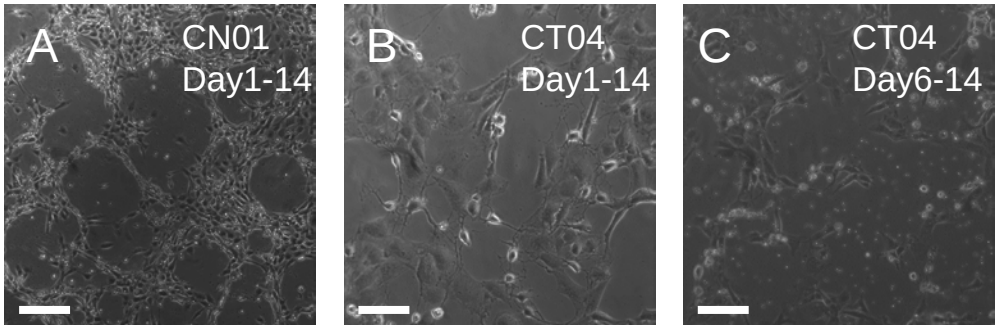

Figure S10. RhoA influences cell morphology. (A-C) Phase-contrast image of cells cultured on MRS for 14 days after seeding in the presence of 1µM CN01 (A). Phase-contrast image of cells cultured for 14 days and treated with 1µM CT04 each day (B). Phase-contrast image of $p190^{KD}$ cells cultured for 14 days and treated with 1µM CT04 every day after 6 days of seeding (C). Scale bar = 20 µm. Images representative of n = 4 cultures for each condition.

Movies S1 to S4. Dynamics of cell network formation from CDC spheroid aggregates. Frame rate for all movies is 10 frames/s, with each frame acquired every 30 min.

Movie S1. On day 6, cells emerge in a radial manner from spheroid-like aggregates, and branch to form closed lacunae.

Movies S2 and S3. On day 7, cells continue to emerge from the aggregates and form denser networks of lacunae. Emerging cells exert force on the semi-adherent aggregates that continue to generate adherent, lacunae-forming cells.

Movies S4. On day 8, the lacunae network remains dynamic and constantly remodels itself.